RESEARCH

Sexually dimorphic gene expression and neurite sensitivity to estradiol in fetal arcuate *Kiss1* cells

Caroline Alfaia[1], Vincent Robert[1], Kevin Poissenot[1], Yves Levern[2], Daniel Guillaume[1], Shel-Hwa Yeo[3], William H Colledge[3] and **Isabelle Franceschini[1]**

[1]PRC, INRA, CNRS, IFCE, Tours University, Nouzilly, France
[2]ISP, INRA, Tours University, Nouzilly, France
[3]Reproductive Physiology Group, Department of Physiology, Development and Neuroscience, University of Cambridge, Cambridge, UK

Correspondence should be addressed to I Franceschini: isabelle.franceschini-laurent@inra.fr

Abstract

Kiss1 neurons of the arcuate (ARC) nucleus form an interconnected network of cells that communicate via neurokinin B (encoded by *Tac2*) and its receptor (encoded by *Tacr3*) and play key roles in the control of the reproductive axis through sex hormone-regulated synthesis and release of kisspeptin peptides (Kp, encoded by *Kiss1*). The aim of this study was to determine whether the *Kiss1* cell population of the ARC already displays sexually dimorphic features at embryonic age E16.5 in mice. At this time of development, *Kiss1*-GFP- and Kp-immunoreactive cell bodies were restricted to the ARC and not found in the pre-optic area (POA). The *Kiss1*-GFP cell population was identical in size between sexes but had significantly lower *Kiss1*, *Tac2*, and *Tacr3* mRNA levels and lower Kp-ir fiber density in the POA in male compared to female fetuses. Receptors for androgen (*Ar*) and estrogen (*Esr1*, *Esr2*, *Gpr30*) and the *Cyp19a1* gene (encoding the estradiol-producing enzyme aromatase) transcripts were also detected in fetal ARC *Kiss1*-GFP cells with significant sex differences for *Ar* (higher in males) and *Esr1* (higher in females). Functional studies on primary cultures of sorted fetal *Kiss1*-GFP cells revealed a significant negative effect of estradiol treatment on neurite outgrowth on the fourth day of culture in the female group specifically. We conclude that the ARC *Kiss1* cell population is already sexually differentiated at E16.5 and that its morphogenetic development may be particularly vulnerable to estradiol exposure at this early developmental time.

Key Words
- kisspeptin neurons
- estradiol
- fetal development
- sexual differentiation
- arcuate nucleus
- morphogenesis

Journal of Endocrinology (2020) **244**, 1–11

Introduction

Kisspeptins (Kp), encoded by the *Kiss1* gene, are short peptides best known to act in the brain as activators of the reproductive axis at puberty via their potent gonadotrophin-releasing hormone (GnRH) secretagogue activity. Noteworthy, they also play neuromodulatory roles on other neuronal populations throughout the brain (Liu & Herbison 2016). Kp are produced by two main populations of *Kiss1* neurons, the cell bodies of which are located in the preoptic area (POA) including the anteroventral periventricular (AVPV) region, and in the arcuate nucleus (ARC) of the hypothalamus with fibers projecting widely throughout the brain (Lehman *et al.* 2013).

The *Kiss1* cell population in the POA is larger in females than in males and plays a determinant role in triggering ovulation (Clarkson & Herbison 2009).

https://joe.bioscientifica.com
https://doi.org/10.1530/JOE-18-0142

In the adult ARC, sex differences in *Kiss1* expression are more subtle than in the POA and only apparent using sensitive techniques such as qRT-PCR (Adachi *et al.* 2007, Knoll *et al.* 2013). In addition, sex differences in the *Kiss1* cell population in the ARC have occasionally been reported at the morphological (Yip *et al.* 2015) and functional levels in adult mice (De Croft *et al.* 2012). This sexual dimorphism may be related to the regulatory role some ARC neurons seem to play in the timing of puberty and the cyclic regulation of GnRH pulses and surges in females (Beale *et al.* 2014, Hu *et al.* 2015, Mittelman-Smith *et al.* 2016).

In this study, we hypothesized that the sexual dimorphism of *Kiss1* neurons in the ARC starts to develop before birth. It was recently shown that *Kiss1* expression in the ARC is turned on very early in the fetal brain (Desroziers *et al.* 2012, Knoll *et al.* 2013). It was therefore possible to isolate ARC *Kiss1* cells by FACS from transgenic fetuses expressing GFP under the control of the endogenous *Kiss1* promoter. Significant transcriptional and morphological sex differences were found in this cell population at E16.5. The discovery of higher levels of *Esr1* in the ARC *Kiss1* cells of female fetuses prompted us to compare the direct estradiol responsiveness of ARC *Kiss1* cells *in vitro* specifically sorted from male and female fetuses.

Materials and methods

Animals

Kiss1-CreGFP mice (Gottsch *et al.* 2011) were obtained from the Jackson Laboratory (Kiss-1$^{tm1.1(Cre/EGFP)Stei}$/J; strain (129S6/SvEvTac x C57BL/6NCr)F1) and bred for over ten generations with C57/Bl6 mice (Charles Rivers). Mice were housed and bred in the INRA rodent facility of Nouzilly (UEPAO, authorization # A37801 from the French ministry of agriculture), in compliance with French and European legislation governing the care and use of laboratory animals (Decree 2013-118 du 1er février 2013; Art. R.214-87-88-89 and Decree 2010/63/UE). Age-matched heterozygous embryos were obtained by mating wild type C57/Bl6 females with homozygous *Kiss1*-CreGFP males for 4 h to overnight. The following morning was considered embryonic day E0.5. *Kiss1*-knockout mice (d'Anglemont de Tassigny *et al.* 2007) and their corresponding wild-type (WT) controls were group housed and bred at the University of Cambridge. Animal handling was carried out with the approval of the Cambridge University Biomedical Services Local Ethics Committee.

Experiment 1: Immunohistochemical characterization of the ARC *Kiss1*-GFP cell population

Tissue preparation for immunohistochemistry

Timed-pregnant mice were killed by cervical dislocation. E16.5 embryos were removed individually by cesarean section. A sample of fetal tissue was collected from each fetus and processed for PCR sexing using primers for *Sry* (5′-ATGGAGGGCCATGTCAAG-3′ and 5′-AACAGGCTGCCAATAAAAGC-3′). The heads were fixed for 24 h at 4°C in 4% paraformaldehyde in 0.1 M phosphate buffer solution, pH 7.4 (PBS), cryoprotected in a 30% sucrose solution and stored at 4°C. Embryonic heads were cut with a cryostat (CM3050S; Leica Microsystems SAS) in the horizontal plane. The ventral forebrain was collected as one set of approximately 80 consecutive 20-µm thick sections that were mounted on gelatin-coated glass slides. The first, most posterior forebrain section collected comprised the interpeduncular fossa and the olfactory bulbs and the last one the median eminence. The slides were stored at −20°C until the immunohistochemistry procedure.

Immunohistochemistry

Slides from all fetuses were processed at the same time using standard immunofluorescent staining procedure with antibodies listed in Table 1. Following counterstaining with Hoechst 33258 (Invitrogen), slides were dipped in a solution of Sudan black 0.3% (Sigma-Aldrich), cover-slipped with Fluoromount-G (SouthernBiotech, Birmingham, AL, USA) and stored at 4°C in the dark until analysis. The specificity of the staining with the anti-GFP antibody was verified on parallel sections from WT embryos. The specificity of the staining with anti-Kp was verified on parallel sections from *Kiss1* KO embryos or after preadsorbtion of the primary antibody with synthetic Kp52 as previously described (Franceschini *et al.* 2013).

Fluorescence microscopy and image acquisitions

All sections were screened for the presence of GFP-immunofluorescent cells using a light microscope (Axio Imager M.2, Carl Zeiss, EC Plan-Neofluar 10×/0.3). The GFP in the transgenic model used is fused to CRE which has a nuclear localization signal. The nuclear localization of the GFP signal, was verified by Hoechst colocalization using higher resolution objectives (EC Plan-Neofluar 20×/0.50 and EC Plan-Neofluar 40×/0.75). The anatomical position of the GFP-ir cells was recorded according to an atlas of the developing mouse brain (Schambra 2008).

https://joe.bioscientifica.com
https://doi.org/10.1530/JOE-18-0142

Table 1 Antibody information.

Peptide/protein target	Antigen sequence (if known)	Name or cat no. of antibody	Manufacturer source	Host species monoclonal or polyclonal	Dilution used
Green fluorescent protein		GFP1020	AVES LAB	Chicken polyclonal	10,000
Kisspeptin	PPVEGPAGRQRPLC	AC053	Alain Caraty INRA	Sheep polyclonal	2000
Chicken IgG		703-545-155	Jackson Immunoresearch	Donkey polyclonal	500
Sheep IgG		713-066-147	Jackson Immunoresearch	Donkey polyclonal	500

Quantitative analysis of GFP/Kp double immunoreactivity in the ARC and of Kp immunoreactivity in the POA were performed on digital images acquired with a spectral LSM780 confocal microscope (Axio Observer Z1, Carl Zeiss, Plan-Apochromat 40×/1.4 Oil DIC M27) on three representative sections sampled throughout the antero-posterior extent of the ARC and on two representative sections sampled at the level of the highest density of Kp-ir fibers in the medial preoptic area, respectively. The Cy3 signal was captured with a specific 560 nm emission filter to reduce noise, enabling unambiguous detection of Kp-ir fibres. On each section through the ARC, one image (x: 103.78 µm, y: 103.78 µm; 500×500 px), including at least 12 GFP-ir cells, was acquired (pinhole open to 0.53 DU), at the xyz level of maximum GFP immunoreactivity. *Kiss1*-GFP cells were considered to be double-labeled Kp when at least two adjacent pixels with gray value above background were recorded for each fluorochrome. On each section through the POA, two images (x: 212.34 µm, y: 212.34 µm; 1024×1024 px) were acquired (pinhole open to 0.53 DU), at the xyz level of maximum Kp immunoreactivity, located 600 µm lateral to the third ventricle border and 200 µm caudal to the rostral limit of the forebrain. Images were binarized after gray level value thresholding over background and the total pixel number was calculated using ImageJ and used as an estimate of Kp-ir fiber density.

Quantitative analysis

One male and one female fetus from each of the three different pregnant mice were used for quantitative analysis. The percentage of GFP/Kp double-immunoreactive cells was calculated as the total number of double-labeled cells over the total number of *Kiss1*-GFP-ir cells. Kp-ir fiber density in the POA was analyzed by variance analysis after logarithmic transformation of the data, with a model totally nested using the procedure *PROC NESTED* in SAS software (SAS Institute Inc.). The model includes the maternal effect and the sex of the fetuses' effect. The effect of the sex of the fetuses was tested with the data from four acquisition fields per fetus on three male–female siblings. Results were reported as arithmetical means ± S.E.M. Statistical differences were considered significant at $P<0.05$.

Fetal MBH cell dissociation and fluorescence-activated cell sorting (FACS) of *Kiss1*-GFP cells (experiments 2 and 3)

E16.5 fetuses were quickly collected and morphologically sexed by macroscopic examination of their gonads. Brains were removed and placed with the ventral surface upward in a small petri dish under a stereomicroscope. A small tissue block including the mediobasal hypothalamus (MBH) was delimited by two lateral cuts lying approximately 350 µm to either side of the midline and one rostral cut behind the optic chiasma using ophthalmic scissors and dissected out with fine curved forceps inserted in the mesencephalic flexure. Depending on the success of overnight matings, two to four pregnant mice were obtained per experiment, and the dissected MBH tissues from all fetuses (originating from the different pregnant mice) were pooled and grouped according to sex prior to cell dissociation and FACS sorting. For cell dissociation, these tissues were briefly chopped with a n°10 scalpel blade before enzymatic digestion in a solution of papain and DNase (Worthington, Lakewood, NJ, USA). Cells were mechanically dissociated via passages through 30G and 27G needles and centrifuged. The pellet was resuspended in a solution of albumin/ovomucoid (1 mg/mL in EBSS buffer) and filtered through 40 µm nylon mesh. Cells were centrifuged at 300 ***g*** for 5 min over a cushion of albumin/ovomucoid (10 mg/mL in EBSS) and resuspended in phenol red-free neurobasal medium supplemented with 2% B-27 (Invitrogen), 1% Glutamax (Gibco) and 10 µg/mL Gentamycin (Sigma-Aldrich). Cell suspensions were maintained on ice until FACS followed by qRT-PCR analysis or cell culture. Dissociated MBH cells were sorted on MoFlo® Legacy or Astria cell sorters (Beckman Coulter), using a blue laser operating at 488 nm. Cells were sorted with 90–100 µm nozzles based on

https://joe.bioscientifica.com
https://doi.org/10.1530/JOE-18-0142

positive fluorescence in the green channel using precisely the same gating parameters for the male and female group of cells. Debris was eliminated based on morphological criteria using forward scatter (FSC) vs side scatter (SSC). The position of the sort window for *Kiss1*-GFP-positive cells was evaluated by comparison with WT mouse green auto-fluorescence.

Experiment 2: Transcriptional characterization of the ARC *Kiss1*-GFP cell population

Quantitative RT-PCR (qRT-PCR)

For each FACS experiment, 500 cells of each group were directly collected in a PCR tube filled with 9 µL of lysis reagent and stored on ice until RT in the same tube as previously described (Ho *et al.* 2013). Quantitative PCR was performed with a qPCR iCycler (iQV3.1 software; BioRad) using Sso advanced SYBR Green Supermix (BioRad). PCR cycling conditions were optimized from previously published protocols using the primers listed in Table 2. The PCR cycle for *Ar*, *Tacr3*, *Esr1* and *Esr2* consisted of a 5-min denaturation step at 95°C, followed by 40 rounds of amplification defined by 10–15 s denaturation at 95°C, 59 s annealing at 55.5–61°C depending on the target, and 10 s extension at 72°C (2 s for *Tacr3*). For *Actbh*, *Polr2a*, *Kiss1*, *Tac2*, *Cyp19a1* and *Gpr30*, PCR samples were first heated 2 min at 50°C and 5 to 10 min at 95°C, followed by 40 cycles of amplification defined by 10–15 s at 95°C and 59 s at 60°C (*Polr2a*, *Cyp19a1* and *Gpr30*) or 60.7°C (*Actbh*, *Kiss1*, *Tac2*). PCR specificity was verified by melting curve analysis and agarose gel electrophoresis. Each sample was run in triplicate to obtain an average cycle threshold value (Ct). Negative control samples devoid of cDNA templates were included for each PCR and yielded no amplification. For each assay, a standard curve was created using a serial dilution of cDNA from a pool of *Kiss1*-GFP sorted cells or from punches of postnatal ARC. PCR efficiencies ranged from 80 to 105% depending on the target gene. A cycle threshold (Ct)-based relative quantification with efficiency correction and normalization to two housekeeping genes (*Actb* and *Polr2a*) was calculated using the software Bio-Rad CFX Manager 3.0.

Statistical analysis

Five independent FACS experiments were included in the analysis of the average number of GFP cells sorted per fetus and gene expression analysis by qRT-PCR. All data are expressed as the mean ± S.E.M. and represented by histograms. Statistical analysis was performed using GraphPad Prism version 5.00 for Windows. Two sample comparisons were performed using paired Wilcoxon or Mann–Whitney tests. Statistical differences were considered significant at $P<0.05$.

Experiment 3: Primary culture of ARC *Kiss1*-GFP cells

Primary cell culture

FACS sorted cells were collected into 500 µL Eppendorf tubes filled with phenol red-free neurobasal medium

Table 2 Primer information.

Target gene	Primer sequence		Amplicon (bp)
Beta actin (*Actb*)	Fwd	TGACCCAGATCATGTTTGAG	159
	Rev	GGAGAGCATAGCCCTCGTAG	
Polypeptide A (*Polr2a*)	Fwd	GCACCACGTCCAATGATAT	267
	Rev	GTGCTGCTGCTTCCATAA	
Kisspeptin (*Kiss1*)	Fwd	AGCTGCTGCTTCTCCTCTGT	118
	Rev	GATTCCTTTTCCCAGGCATT	
Neurokinin B (*Tac2*)	Fwd	TTCCACAGAAACGTGACATGC	101
	Rev	GGGGGTGTTCTCTTCAACCAC	
Tachykinin receptor 3 (*Tacr3*)	Fwd	CCAACTACTGCCGCTTCCA	272
	Rev	GAAATGTTGCTTGGGACCTTCT	
Estrogen receptor alpha (*Esr1*)	Fwd	CGTGTGCAATGACTATGCCTCT	128
	Rev	TGGTGCATTGGTTTGTAGCTGG	
Androgen receptor (*Ar*)	Fwd	GGCGGTCCTTCACTAATGTCAACT	142
	Rev	TGGAGCCATCCAAACTCTTGAGAC	
Cytochrome P450 (*Cyp19a1*)	Fwd	TGTGTTGACCCTCATGAGACA	190
	Rev	CTTGACGGATCGTTCATACTTTC	
Estrogen receptor beta (*Esr2*)	Fwd	GTCAGGCACATCAGTAACAAGGG	96
	Rev	ATTCAGCATCTCCAGCAGCAGGTC	
G-protein-coupled estrogen receptor 1 (*Gpr30*)	Fwd	GTGGCCAAGCCTCAACACTCAC	103
	Rev	GGTGGACAGGGTGTCTGATGTCTG	

https://joe.bioscientifica.com
https://doi.org/10.1530/JOE-18-0142

supplemented with 2% B-27, 1% Glutamax (Gibco), 10 µg/mL Gentamycin (Sigma-Aldricht), 10% charcoal-stripped FBS and 20 ng/mL FGF2 (PreproTech). Cells were seeded on poly-ornithine-laminin-coated glass multi-well slides (Lab-tek chamber slide system, 8 wells, Nunc) at a density of 300 cells in 30 µL at the center of each well and allowed to settle for 2 h in a 37°C, 5% CO_2 incubator. 300 µL of the same medium were then added to each well. Twenty-four hours after seeding, the entire medium was replaced by FBS-free medium with or without 100 pM 17-β-estradiol (E_2, Sigma-Aldrich).

Time-lapse recording

From 2 to 4 days in culture (DIV), cells were incubated under a LSM780 confocal microscope (Axio Observer Z1, Carl Zeiss) equipped with a culture chamber at 37°C in 5% CO_2. Digital image tiles of each well were recorded in transillumination every 6 h using a ×20 objective (Plan-Neofluar 20×/0.50 M27).

Morphological analysis

Operators were blind to treatment or sex, all refractive cells were manually counted on images recorded 25, 55 and 85 h after cell seeding (DIV2, DIV3 and DIV4, respectively) using the cell counter plug-in of ImageJ (NIH). Neurite lengths were manually measured using the segmented line measurement of ImageJ. Neurons contacting each other or bypassing the acquisition field were excluded from the analysis.

Statistical analysis

Five independent FACS/primary culture experiments were included in the analysis of the average number of GFP cells detected per fetus and of the number of adherent cells at DIV2. Two sample comparisons between male and female were performed using paired Wilcoxon and Mann–Whitney tests with GraphPad Prism, version 5.00 for Windows. Three experiments were followed by time lapse from DIV2 to DIV4. For each culture, experimental group and timepoint, neurites from all distinct neurite-bearing cells were measured. Multiple comparisons between time, sex and treatment groups were performed using three-factor repeated-measures ANOVA on Statistica, version 10.00 with sex and treatment as independent factors. When applicable, Fisher's least significant difference *post hoc* comparisons were used to determine statistical differences between groups of interest. All data are expressed as the mean ± S.E.M. and represented by histograms. Statistical differences were considered significant at $P<0.05$.

Results

Experiment 1: Similar GFP and Kp immunoreactivity in the ARC of male and female fetuses but higher Kp-ir fiber density in the POA of female fetuses

Kiss1-GFP-ir cells were distributed along the entire antero-posterior extent of the fetal ARC, positioned bilaterally on the ventral sides of the third ventricle, from the level of the infundibular recess to the mammillary recess in both male and female fetuses (Fig. 1A). Counterstaining with Hoechst enabled verification that the GFP protein which carries a nuclear localization sequence was confined to cell nuclei. *Kiss1*-GFP neurons were not found in the other ventral forebrain areas where *Kiss1* expression has been described in adults including the POA, dorsomedial nucleus and medial amygdala. The majority of *Kiss1*-GFP cells were concentrated in a small ARC area just above the developing pituitary. Their density appeared similar between males and females (Fig. 1B and C). In female and male fetuses, the majority of the GFP+ cells also expressed Kp (80 ± 8% in females and 81 ± 8% in males; Fig. 1B and C respectively). The specificity of the Kp immunolabeling was confirmed by the absence of staining in the ARC of age-matched *Kiss1* KO fetuses, in contrast to the clear Kp immunofluorescent signal detected in the ARC of WT counterparts (data not shown). Scattered Kp-ir fibers were detected in the lateral and medial POA of both male and female fetuses, where these appeared to concentrate in a small region anterior to the preoptic nucleus and ventral to the bed nucleus of the stria terminalis (Fig. 1A′). There was no significant maternal effect, but there was a significant effect of fetal sex on Kp-ir density which was on average two-fold higher in female than male fetuses at this stage of pregnancy ($P=0.018$, Fig. 1D, E and F).

Experiment 2: Sex differences in the transcriptional profile of E16.5 ARC *Kiss1*-GFP cells

This experiment was designed to investigate the possible sex differences in the transcriptional profile of the *Kiss1*-GFP cell population of the fetal ARC at the time of the male-specific prenatal (E16.5) testosterone surge. We focused on transcripts playing key roles in the maturation of reproductive function and previously identified in adult ARC *Kiss1* cells. These included *Kiss1*, *Tac2*, *Esr1* and *Ar*. Figure 2A displays the position of the sort window for *Kiss1*-GFP-positive cells, which was set by comparison with WT mouse green auto-fluorescence (Fig. 2B).

https://joe.bioscientifica.com
https://doi.org/10.1530/JOE-18-0142

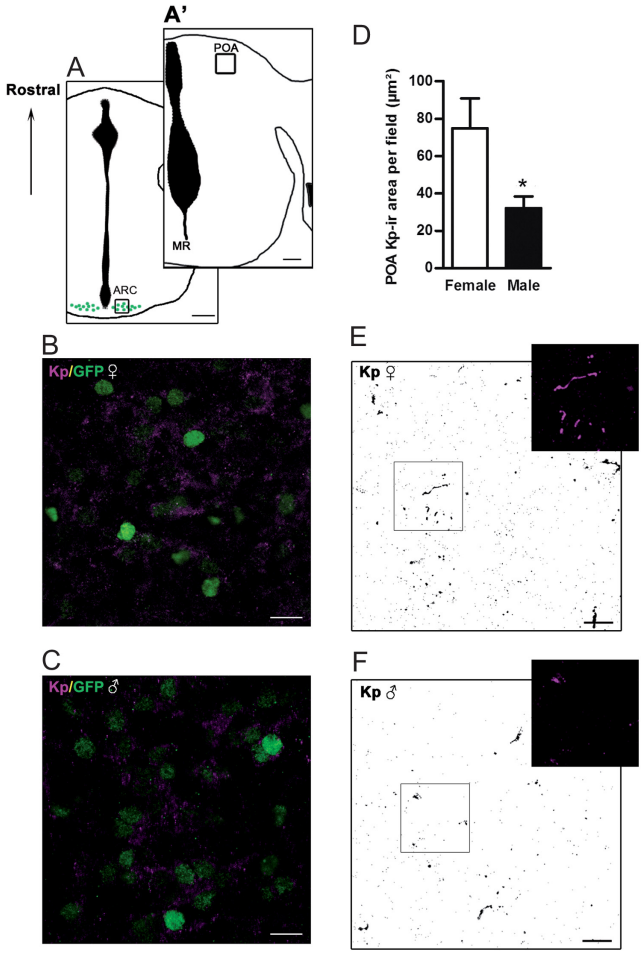

Figure 1
GFP and Kp immunoreactivity in the ARC and rostral POA of E16.5 male and female brains. Schematic drawings of two horizontal sections through the ventral forebrain at the level of the arcuate nucleus (A) and preoptic area (A′), illustrating the restricted localization of *Kiss1*-GFP cells in the ARC. (B and C) Representative confocal optical sections scanned at the level of the boxed area in (A), illustrating Kp (magenta) and GFP (green) immunoreactivity in the arcuate nucleus of a female and male brain respectively. Note that the density of GFP-immunoreactive cell nuclei was undistinguishable between males and females and that most were apposed to Kp immunoreactivity in males as in females. (D) Quantitative analysis (mean ± S.E.M. of Kp immunoreactive surface area per field in the area of the POA illustrated by the squared box in A′. Nested ANOVA detected a significant effect of sex, $*P < 0.05$. (E and F) Representative binarized confocal optical sections scanned at the level of the boxed area in (A′), illustrating Kp (black) immunoreactivity in the rostral POA of female (E) and male (F) fetuses. A representative illustration of Kp-immunofluorescent fibers (magenta) is displayed in the top right corner of each binarized image. The lateral and third ventricle are filled in black. Arc, arcuate nucleus; MR, mammillary recess; POA, preoptic area. Scale bars: 200 µm (A and A′); 20 µm (B); 10 µm (D and E).

The average number of GFP+ sorted cells per ARC was not statistically different between male and female fetuses (female 170±41.7 and male 175.3±36.4 GFP+ cells per ARC, $P=0.63$) consistent with our IHC data. *Kiss1* mRNA levels were significantly enriched in the population of

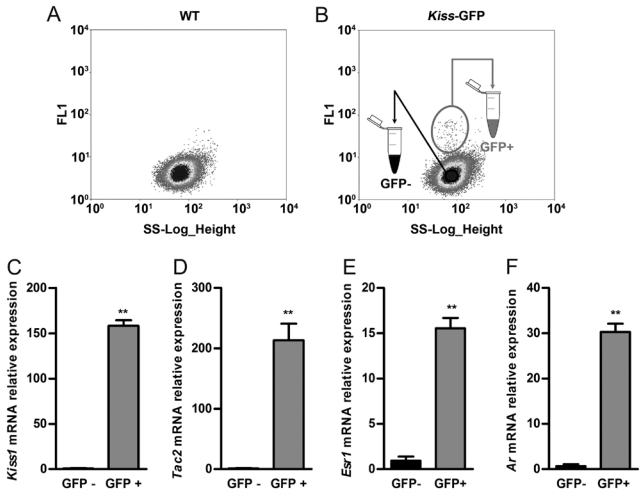

Figure 2
Enrichment in *Kiss1*, *Tac2*, *Esr1* and *Ar* transcripts in *Kiss1*-GFP cells sorted from E16.5 ARC. Representative FACS profiles (FL1/SSC) from a pool of wild type (A) and *Kiss1*-GFP (B) fetal MBH cell suspension, displaying in B the sort windows for GFP⁻ (black circle) and GFP+ (gray circle) cells. The specificity of the GFP+ sort window in B is attested by the absence of events in this area in A. Histograms display quantitative analysis of *Kiss1* (C), *Tac2* (D), *Esr1* (E) and *Ar* (F) mRNA levels as measured in the sorted cell populations by RT-qPCR (mean ± S.E.M). Data are expressed as fold change in relative expression with GFP⁻ cell sorts arbitrary set at 1. All transcripts were significantly enriched in GFP+ cells as compared to GFP cells. Mann–Whitney test, $**P < 0.01$.

GFP+ sorted cells compared to the GFP⁻ sorted one (150-fold higher, $P<0.01$) (Fig. 2C). GFP+ sorted cells also expressed 200-fold more *Tac2* transcripts ($P<0.01$) (Fig. 2D), 15-fold more *Esr1* transcripts ($P<0.01$) (Fig. 2E) and 30-fold more *Ar* transcripts ($P<0.01$) than the GFP⁻ cells (Fig. 2F). Significant sex differences were detected among the GFP+ sorted cells: *Kiss1*, *Tac2 and Tacr3* mRNA levels were significantly lower in the male compared to the female *Kiss1*-GFP cell population ($P<0.05$) (Fig. 3A, B and C respectively). Significant sex differences were also detected in *Esr1* and *Ar* transcript levels, which were respectively lower and higher in the male compared to the female *Kiss1*-GFP cell population ($P<0.05$) (Fig. 3D and E respectively). *Gpr30*, encoding a membrane anchored GPCR estrogen receptor, and *Esr2*, encoding estrogen receptor beta and *Cyp19a1*, encoding aromatase, were detected in male and female GFP-sorted cells but could not be quantitatively compared between sexes due to low detection levels (data not shown).

Experiment 3: Morphogenetic response of cultured *Kiss1*-GFP neurons to estradiol

The differences observed in the level of *Esr1* expression between the male and female *Kiss1*-GFP cell populations

https://joe.bioscientifica.com
https://doi.org/10.1530/JOE-18-0142

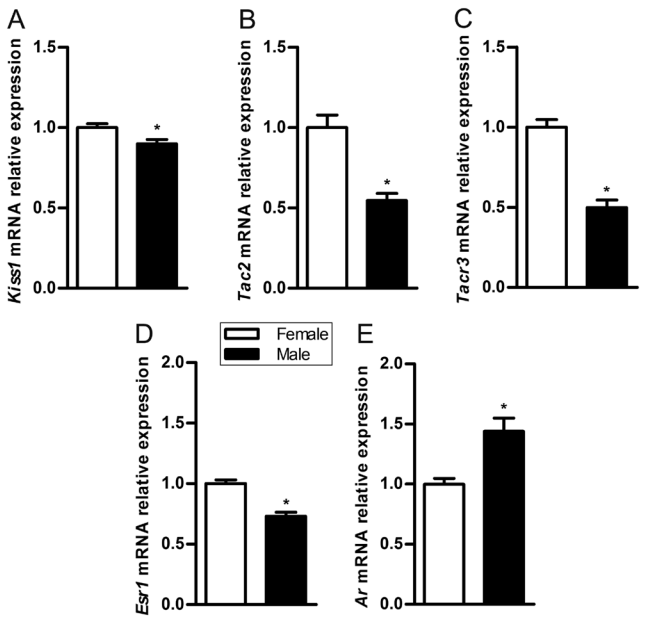

Figure 3
Sex differences in *Kiss1*, *Tac2*, *Tacr3*, *Esr1* and *Ar* mRNA levels in *Kiss1*-GFP cells sorted from E16.5 ARC. Histograms display quantitative analysis of *Kiss1* (A), *Tac2* (B), *Tacr3* (C), *Esr1* (D) and *Ar* (E) relative mRNA levels in sorted *Kiss1*-GFP cells as measured by RT-qPCR (mean ± S.E.M., expressed as fold change in relative expression with values for *Kiss1*-GFP cells sorted from the female ARC arbitrary set at 1). Mann–Whitney tests revealed significant sex differences for each transcript, with females expressing higher levels of *Kiss1*, *Tac2*, *Tacr3* and *Esr1* and lower levels of Ar than their male siblings. Mann–Whitney test, $*P < 0.05$.

(Experiment 2) suggested that the response of this cell population to estradiol could differ between sexes at this early developmental stage. During fetal development, estradiol is known to influence neuronal survival and axonal growth in different cell populations (McCarthy 2008). Since these effects can conveniently be studied *in vitro* (de Lacalle 2006), we developed a culture system where FACS sorted *Kiss1*-GFP cells grew neurites for several days *in vitro* (Fig. 4A, B and C). This enabled investigation of estradiol's morphogenetic effects on this parameter. The average number of GFP+-sorted cells per fetal MBH was not statistically different between sexes (female 354.6±42.7 and male 347.8±39.87 GFP+ cells per ARC; $P=0.81$). A significant sex difference was detected in the number of healthy adhered cells per well at 2 days of culture (DIV2) ($P<0.05$) (Fig. 4D). The mean cell density was 9±1 cells/mm^2 in female and 11±1 cells/mm^2 in male cultures. For all experimental groups, the majority of surviving neurons extended one single neurite. Neurites generally grew along non-linear routes as illustrated in Fig. 4C and sometimes contacted each other by the fourth day.

Three-way ANOVA detected a significant effect of time on neurite initiation but did not detect any effect of treatment nor sex on this parameter (Fig. 4E). *Post hoc* analysis revealed a significant increase in the number of cells with neurites between DIV2 and DIV3 in the female groups regardless of treatment and in the untreated male group (Fig. 4E). The number of cells with primary neurites remained stable between DIV3 and DIV4 for all experimental conditions. Three-way ANOVA detected a significant increase of neurite length with time ($P<0.001$) and an interaction of time with treatment ($P<0.05$) (Fig. 4F). At DIV4, estradiol-treated female cultures had significantly shorter neurites than their control counterpart ($P=0.02$). Estradiol-treated male cultures also displayed on average shorter neurites than controls but the difference did not reach statistical significance ($P=0.28$).

Discussion

This is the first study to show that *Kiss1* neurons in the ARC region of the hypothalamus show clear sexual dimorphisms at E16.5 of fetal development, in terms of transcription of major genes important for reproduction, morphology and *in vitro* direct morphogenetic response to estradiol.

Immunohistochemical analysis of the ventral forebrain did not detect any *Kiss1*-GFP neurons anywhere other than the ARC at this fetal stage, even after immunohistochemical amplification of the GFP signal. This is consistent with previous reports using *in situ* hybridization or other mice lines reporting *Kiss1* promoter activity to map *Kiss1* cells in fetal brains (Knoll *et al.* 2013, Kumar *et al.* 2014, 2015). In addition, 80% of the GFP+ cells also expressed Kp for both sexes. We are therefore confident that fluorescence-activated cell sorting of the GFP+ cells isolated predominantly the *Kiss1* neurons of the ARC. The efficiency of this sorting procedure was attested by the 150-fold enrichment in *Kiss1* transcripts in the GFP+ fraction of cells. We provide here the first evidence that fetal ARC *Kiss1* cell population already co-expresses *Tac2* and *Tacr3*, which is very early compared to other cell populations of the MBH. There is evidence for an autocrine/paracrine communication between ARC *Kiss1* neurons via neurokinin B in adults (Navarro *et al.* 2009, Krajewski *et al.* 2010). It is therefore conceivable that some ARC *Kiss1* neurons already communicate locally via neurokinin B in the fetal brain and that this

https://joe.bioscientifica.com
https://doi.org/10.1530/JOE-18-0142

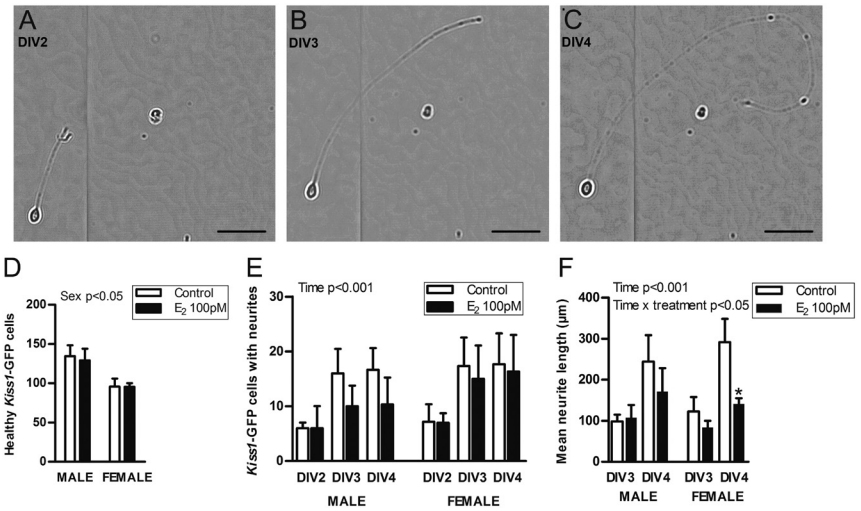

Figure 4
Morphogenetic effects of estradiol on primary cultures of ARC *Kiss1*-GFP cells sorted from male and female E16.5 ARC. Bright field photomicrographs of a sorted cell on the second (DIV2, A), third (DIV3, B) and fourth day *in vitro* (DIV4, C), illustrating neurite outgrowth. (D) Quantitative analysis of the number of healthy adhered *Kiss1*-GFP cells per culture at DIV2 as a function of sex and estradiol (E2, 100 pM) treatment. Two-way ANOVA detected a significant effect of sex on cell survival at DIV2. (E and F) Quantitative analysis of respectively the number of neurite-bearing *Kiss1*-GFP cells per culture and neurite length, as a function of sex, culture time and E2 treatment. Three-way ANOVA detected a significant effect of culture time on neurite initiation and a significant effect of time and interaction between time and treatment on neurite length. *Post hoc* Fisher's least significant difference test, $*P < 0.05$ compared with control female at DIV4. Scale bar: 10 µm.

communication plays an active role in the early stages of maturation of the reproductive axis (Gianetti *et al.* 2010).

Significant sex differences among the E16.5 ARC *Kiss1*-GFP neurons were detected for various parameters. For instance, *Kiss1* mRNA levels were 10% lower in the male population of sorted *Kiss1*-GFP cells. In contrast, FACS and immunohistochemical analyses were unable to detect any significant sex difference in the average number and density of ARC *Kiss1*-GFP cell bodies per fetus. This discrepancy is consistent with a previous report (Knoll *et al.* 2013) and probably reflects the higher sensitivity of qPCR over the quantification of reporter fluorescent molecule or indirect immunohistochemical labeling for gene expression analysis. It implies that the size of the ARC *Kiss1* population does not differ between sexes but that *Kiss1* mRNA levels per cell are on average lower in male than female fetuses at this developmental stage. This differs from the sexual dimorphism detected a few days later in the fetal POA where the size of the kisspeptin cell population was clearly higher in male than female fetuses (Clarkson *et al.* 2014). In addition, significant sex differences were detected in the levels of *Tac2* and *Tacr3* transcripts in the fetal ARC *Kiss1* cell population. Both were also lower in the population of *Kiss1*-GFP cells sorted from male fetuses, suggesting reduced neurokinin B signaling between ARC *Kiss1* cells in male compared to female fetuses. The sex differences in the wiring and regulation of ARC neurokinin B cells that have been identified postnatally (Ciofi *et al.* 2006, Kauffman *et al.* 2009) may thus have a fetal origin.

In the ARC of adult mice, *Kiss1*, *Tac2* and *Tacr3* are under acute downregulation by circulating estradiol and testosterone (Smith *et al.* 2005*a*,*b*, Navarro *et al.* 2009, 2011). However, whether these genes are already regulated by gonadal hormones prior to birth is not yet clear. Genetic studies in mice suggest a role for gonadal factors in the regulation of *Kiss1* expression in the MBH of E17 fetuses (Knoll *et al.* 2013). Interestingly, our gene expression analysis revealed a considerable enrichment of *Esr1* and *Ar* transcripts within ARC *Kiss1*-GFP cells as compared to the other cell populations of the E16.5 MBH. This result reinforces previous indirect immunohistochemical data that most ARC *Kiss1* cells could already synthesize ERα and AR proteins by E16.5 (Kumar *et al.* 2014, 2015). Hence, ARC *Kiss1* cells may already be a primary direct target of sex steroids in the fetus. In male fetuses, *Kiss1*, *Tac2* and *Tacr3* downregulation by sex steroid receptor signaling in the ARC could possibly contribute to a negative feedback regulation by circulating testosterone on LH secretion at the end of fetal life (Pointis *et al.* 1980). Noteworthy, we also detected significant sex differences in *Esr1* and *Ar* mRNA levels within the sorted *Kiss1*-GFP cells (being respectively higher and lower in females than males). As described in other embryonic neural cell systems, this sex difference may be the result of an interaction between gonadal hormones, neuronal derived estradiol and sex chromosome complement (Young & Chang 1998, Cambiasso *et al.* 2017). As a consequence, the sensitivity and responses of these cells to steroids during early development is likely to differ between males and females. Later in life, a similar sex difference in sex steroid receptor expression appears to develop in the *Kiss1* cell population of the POA (Poling *et al.* 2017).

Beyond their action on gene transcription, sex steroids, in particular, estrogens can also exert important morphogenetic actions on developing brain structures

https://joe.bioscientifica.com
https://doi.org/10.1530/JOE-18-0142

(McCarthy 2008). We therefore sought to compare the distribution of ARC *Kiss1*-GFP neurons and Kp-ir fibers between male and female fetuses. It is unlikely that the Kp-ir fibers detected originated from *Kiss1* neurons in regions other than the ARC since there is no evidence for *Kiss1* expression elsewhere in the brain at this early fetal stage (Knoll *et al.* 2013, Kumar *et al.* 2014, 2015 and present study). A very small amount of Kp-ir cell bodies have been detected in the POA prenatally, but at later fetal stages (Desroziers *et al.* 2012, Clarkson *et al.* 2014). Kp-ir fibers were more abundant in females than male fetuses in the POA, despite similar numbers of *Kiss1*-GFP cells and similar amount of Kp immunoreactivity in the ARC between sexes, as revealed by FACS analysis and immunohistochemistry. This region of the developing POA, located at the rostrolateral border of the medial preoptic nucleus, appears to correspond to a portion of the medial forebrain bundle (MFB) (Schambra 2008). These fetal *Kiss1* fibers may be *en route* toward various forebrain regions where ARC *Kiss1* neurons are known to project in adulthood (Yip *et al.* 2015). Another research group, using genetically engineered mice with a Tdtomato reporter of *Kiss1*-cre activity showed the presence of Tdtomato fibers in the POA of female fetuses but not male fetuses, despite similar numbers of Tdtomato cell bodies, restricted to the ARC (Kumar *et al.* 2014, 2015). Taken together, these results suggest that some ARC *Kiss1* neurons already project to the rostral POA during fetal life and are more abundant in females. This adds to the growing list of sexually dimorphic features observed prenatally in this ventral forebrain area (Henderson *et al.* 1999, Wolfe *et al.* 2005). These few rostral projections may have been missed in a previous tract-tracing study using DiI on fixed neonatal brains that suggested that ARC projection pathways toward the POA establish postnatally via a predominant periventricular pathway and are not sexually dimorphic (Bouret *et al.* 2004). The early ARC rostral Kp projections suggested by the present study may correspond to the recently identified ARC neurokinin B fibers mapped in adult rats along the ventral hypothalamic tract and medial forebrain bundle (Krajewski *et al.* 2010), two fiber tracts which course more laterally and develop prenatally (Altman & Bayer 1978, Goldsmith & Song 1987). In summary, results from gene expression analysis on sorted *Kiss1*-GFP cells and from Kp immunohistochemistry on fetal brains suggest that the ARC population of *Kiss1* cells is prenatally wired and directly responsive to androgens and estrogens in a sex-specific way.

We started to investigate this hypothesis by testing the direct morphological responsiveness of these neurons to exposure to a low dose of estradiol (100 pM) *in vitro*. We successfully set up culture conditions that allowed survival and neurite outgrowth of sorted *Kiss1*-GFP neurons for several days. This culture system is thus very useful to study morphogenetic effects induced by estradiol on *Kiss1* neurons, as opposed to the previously described immortalized *Kiss1* cell lines which do not show signs of morphological differentiation *in vitro* and are rather best suited for molecular investigations (Jacobs *et al.* 2016, Treen *et al.* 2016). A significant sex difference, in favor of males, was detected in the number of cells that adhered and survived 24 h after FACS, adding further evidence of a sex difference in the biological properties of ARC *Kiss1* cells in the fetus. How this observation relates to the transcriptional or morphological sex differences observed *in vivo* remains to be explored. Although ANOVA was not able to detect any significant effect of sex on the neurite outgrowth inhibitory response to 100 pM estradiol, only *Kiss1* cells sorted from female fetuses displayed a significant decrease in neurite outgrowth on the fourth day of culture as compared to their untreated control counterparts (Fisher LSD, $P<0.05$). This may be related to the higher expression of *Esr1* among the female *Kiss1* cell population. In the same vein, a higher vulnerability of female fetuses to exogeneous estrogenic compounds affecting hypothalamic functions has previously been reported (Rebuli & Patisaul 2016).

In conclusion, this study demonstrates sex differences in *Kiss1*, *Tac2*, *Tacr3*, *Esr1* and *Ar* mRNA levels within fetal ARC *Kiss1* cells and in Kp-ir fiber density in the POA, suggesting that male and female ARC *Kiss1* neurons are already differently wired and prone to respond in different ways to sex steroids in the fetus. We developed a primary culture system of purified fetal ARC *Kiss1* cells which directly responded to 100 pM estradiol by decreased neurite outgrowth over culture time. Further studies are however needed to fully explore a possible sex effect in this response and to decipher the precise mechanism of action of estrogens on fetal ARC *Kiss1* cells.

Declaration of interest

The authors declare that there is no conflict of interest that could be perceived as prejudicing the impartiality of the research reported.

Funding

This work was supported by grants from ANR (ANR-15-CE20-0015-01) and BBRC (BB/K003178/). C A was recipient of PhD fellowships from the University of Tours and from the Fondation pour la Recherche Medicale (FDT20160736471).

https://joe.bioscientifica.com
https://doi.org/10.1530/JOE-18-0142

Author contribution statement

C A and I F designed the experiments. C A, V R, K P, Y L, and S Y performed experiments. C A, V R, K P, Y L, D G, S-H Y, W H C, and I F analyzed the experiments. C A and I F wrote the paper.

Acknowledgments

The authors thank Claude Cahier, Déborah Crespin, and Aurélie Sauvage from the UEPAO animal facility for taking care of the animals and Victoria Kyle for tail PCR genotyping of the fetuses. This work has benefited from the facilities and expertise of the 'Plateforme d'Imagerie Cellulaire'/Cell imaging platform (PIC) of the UMR PRC and they are particularly grateful to Marie-Claire Blache for her expert assistance in spectral confocal microscopy, time lapse acquisitions and image analysis.

References

Adachi S, Yamada S, Takatsu Y, Matsui H, Kinoshita M, Takase K, Sugiura H, Ohtaki T, Matsumoto H, Uenoyama Y, *et al*. 2007 Involvement of anteroventral periventricular metastin/kisspeptin neurons in estrogen positive feedback action on luteinizing hormone release in female rats. *Journal of Reproduction and Development* **53** 367–378. (https://doi.org/10.1262/jrd.18146)

Altman J & Bayer SA 1978 Development of the diencephalon in the rat. II. Correlation of the embryonic development of the hypothalamus with the time of origin of its neurons. *Journal of Comparative Neurology* **182** 973–993. (https://doi.org/10.1002/cne.901820512)

Beale KE, Kinsey-Jones JS, Gardiner JV, Harrison EK, Thompson EL, Hu MH, Sleeth ML, Sam AH, Greenwood HC, McGavigan AK, *et al*. 2014 The physiological role of arcuate kisspeptin neurons in the control of reproductive function in female rats. *Endocrinology* **155** 1091–1098. (https://doi.org/10.1210/en.2013-1544)

Bouret SG, Draper SJ & Simerly RB 2004 Formation of projection pathways from the arcuate nucleus of the hypothalamus to hypothalamic regions implicated in the neural control of feeding behavior in mice. *Journal of Neuroscience* **24** 2797–2805. (https://doi.org/10.1523/JNEUROSCI.5369-03.2004)

Cambiasso MJ, Cisternas CD, Ruiz-Palmero I, Scerbo MJ, Arevalo MA, Azcoitia I & Garcia-Segura LM 2017 Interaction of sex chromosome complement, gonadal hormones and neuronal steroid synthesis on the sexual differentiation of mammalian neurons. *Journal of Neurogenetics* **31** 300–306. (https://doi.org/10.1080/01677063.2017.1390572)

Ciofi P, Leroy D & Tramu G 2006 Sexual dimorphism in the organization of the rat hypothalamic infundibular area. *Neuroscience* **141** 1731–1745. (https://doi.org/10.1016/j.neuroscience.2006.05.041)

Clarkson J & Herbison AE 2009 Oestrogen, kisspeptin, GPR54 and the pre-ovulatory luteinising hormone surge. *Journal of Neuroendocrinology* **21** 305–311. (https://doi.org/10.1111/j.1365-2826.2009.01835.x)

Clarkson J, Busby ER, Kirilov M, Schutz G, Sherwood NM & Herbison AE 2014 Sexual differentiation of the brain requires perinatal kisspeptin-GnRH neuron signaling. *Journal of Neuroscience* **34** 15297–15305. (https://doi.org/10.1523/JNEUROSCI.3061-14.2014)

d'Anglemont de Tassigny X, Fagg LA, Dixon JPC, Day K, Leitch HG, Hendrick AG, Zahn D, Franceschini I, Caraty A, Carlton MBL, *et al*. 2007 Hypogonadotropic hypogonadism in mice lacking a functional Kiss1 gene. *PNAS* **104** 10714–10719. (https://doi.org/10.1073/pnas.0704114104)

De Croft S, Piet R, Mayer C, Mai O, Boehm U & Herbison AE 2012 Spontaneous kisspeptin neuron firing in the adult mouse reveals marked sex and brain region differences but no support for a direct role in negative feedback. *Endocrinology* **153** 5384–5393. (https://doi.org/10.1210/en.2012-1616)

de Lacalle S 2006 Estrogen effects on neuronal morphology. *Endocrine* **29** 185–190. (https://doi.org/10.1385/ENDO:29:2:185)

Desroziers E, Droguerre M, Bentsen AH, Robert V, Mikkelsen JD, Caraty A, Tillet Y, Duittoz A & Franceschini I 2012 Embryonic development of kisspeptin neurones in rat. *Journal of Neuroendocrinology* **24** 1284–1295. (https://doi.org/10.1111/j.1365-2826.2012.02333.x)

Franceschini I, Yeo SH, Beltramo M, Desroziers E, Okamura H, Herbison AE & Caraty A 2013 Immunohistochemical evidence for the presence of various kisspeptin isoforms in the mammalian brain. *Journal of Neuroendocrinology* **25** 839–851. (https://doi.org/10.1111/jne.12069)

Gianetti E, Tusset C, Noel SD, Au MG, Dwyer AA, Hughes VA, Abreu AP, Carroll J, Trarbach E, Silveira LFG, *et al*. 2010 TAC3/TACR3 mutations reveal preferential activation of gonadotropin-releasing hormone release by neurokinin B in neonatal life followed by reversal in adulthood. *Journal of Clinical Endocrinology and Metabolism* **95** 2857–2867. (https://doi.org/10.1210/jc.2009-2320)

Goldsmith PC & Song T 1987 The gonadotropin releasing hormone containing ventral hypothalamic tract in the fetal rhesus monkey (*Macaca mulatto*). *Journal of Comparative Neurology* **257** 130–139. (https://doi.org/10.1002/cne.902570110)

Gottsch ML, Popa SM, Lawhorn JK, Qiu J, Tonsfeldt KJ, Bosch MA, Kelly MJ, Rønnekleiv OK, Sanz E, McKnight GS, *et al*. 2011 Molecular properties of kiss1 neurons in the arcuate nucleus of the mouse. *Endocrinology* **152** 4298–4309. (https://doi.org/10.1210/en.2011-1521)

Henderson RG, Brown AE & Tobet SA 1999 Sex differences in cell migration in the preoptic area/anterior hypothalamus of mice. *Journal of Neurobiology* **41** 252–266. (https://doi.org/10.1002/(SICI)1097-4695(19991105)41:2<252::AID-NEU8>3.0.CO;2-W)

Ho V, Yeo SY, Kunasegaran K, De Silva D, Tarulli GA, Voorhoeve PM & Pietersen AM 2013 Expression analysis of rare cellular subsets : direct RT-PCR on limited cell numbers obtained by FACS or soft agar assays. *BioTechniques* **54** 208–212. (https://doi.org/10.2144/000114019)

Hu MH, Li XF, McCausland B, Li SY, Gresham R, Kinsey-Jones JS, Gardiner JV, Sam AH, Bloom SR, Poston L, *et al*. 2015 Relative importance of the arcuate and anteroventral periventricular kisspeptin neurons in control of puberty and reproductive function in female rats. *Endocrinology* **156** 2619–2631. (https://doi.org/10.1210/en.2014-1655)

Jacobs DC, Veitch RE & Chappell PE 2016 Evaluation of immortalized AVPV- and arcuate-specific neuronal kisspeptin cell lines to elucidate potential mechanisms of estrogen responsiveness and temporal gene expression in females. *Endocrinology* **157** 3410–3419. (https://doi.org/10.1210/en.2016-1294)

Kauffman AS, Navarro VM, Kim J, Clifton DK & Steiner RA 2009 Sex differences in the regulation of Kiss1/NKB neurons in juvenile mice: implications for the timing of puberty. *American Journal of Physiology: Endocrinology and Metabolism* **297** E1212–E1221. (https://doi.org/10.1152/ajpendo.00461.2009)

Knoll JG, Clay CM, Bouma GJ, Henion TR, Schwarting GA, Millar RP & Tobet SA 2013 Developmental profile and sexually dimorphic expression of kiss1 and kiss1r in the fetal mouse brain. *Frontiers in Endocrinology* **4** 140. (https://doi.org/10.3389/fendo.2013.00140)

Krajewski SJ, Burke MC, Anderson MJ, Mcmullen NT & Rance NE 2010 Forebrain projections of arcuate neurokinin B neurons demonstrated by anterograde tract-tracing and monosodium glutamate lesions in the rat. *Neuroscience* **166** 680–697. (https://doi.org/10.1016/j.neuroscience.2009.12.053)

Kumar D, Freese M, Drexler D, Hermans-Borgmeyer I, Marquardt A & Boehm U 2014 Murine arcuate nucleus kisspeptin neurons communicate with GnRH neurons in utero. *Journal of Neuroscience* **34** 3756–3766. (https://doi.org/10.1523/JNEUROSCI.5123-13.2014)

Kumar D, Periasamy V, Freese M, Voigt A & Boehm U 2015 In utero development of kisspeptin/GnRH neural circuitry in male mice. *Endocrinology* **156** 3084–3090. (https://doi.org/10.1210/EN.2015-1412)

Lehman MN, Hileman SM & Goodman RL 2013 Neuroanatomy of the kisspeptin signaling system in mammals: comparative and developmental aspects. *Advances in Experimental Medicine and Biology* **784** 27–62. (https://doi.org/10.1007/978-1-4614-6199-9_3)

Liu X & Herbison AE 2016 Kisspeptin regulation of neuronal activity throughout the central nervous system. *Endocrinology and Metabolism* **31** 193–205. (https://doi.org/10.3803/EnM.2016.31.2.193)

McCarthy MM 2008 Estradiol and the developing brain. *Physiological Reviews* **88** 91–124. (https://doi.org/10.1152/physrev.00010.2007)

Mittelman-Smith MA, Krajewski-Hall SJ, McMullen NT & Rance NE 2016 Ablation of KNDy neurons results in hypogonadotropic hypogonadism and amplifies the steroid-induced lh surge in female rats. *Endocrinology* **157** 2015–2027. (https://doi.org/10.1210/en.2015-1740)

Navarro VM, Gottsch ML, Chavkin C, Okamura H, Clifton DK & Steiner RA 2009 Regulation of gonadotropin-releasing hormone secretion by kisspeptin/dynorphin/neurokinin B neurons in the arcuate nucleus of the mouse. *Journal of Neuroscience* **29** 11859–11866. (https://doi.org/10.1523/JNEUROSCI.1569-09.2009)

Navarro VM, Gottsch ML, Wu M, García-Galiano D, Hobbs SJ, Bosch MA, Pinilla L, Clifton DK, Dearth A, Ronnekleiv OK, *et al*. 2011 Regulation of NKB pathways and their roles in the control of Kiss1 neurons in the arcuate nucleus of the male mouse. *Endocrinology* **152** 4265–4275. (https://doi.org/10.1210/en.2011-1143)

Pointis G, Latreille MT & Cedard L 1980 Gonado-pituitary relationships in the fetal mouse at various times during sexual differentiation. *Journal of Endocrinology* **86** 483–488. (https://doi.org/10.1677/joe.0.0860483)

Poling MC, Luo EY & Kauffman AS 2017 Sex differences in steroid receptor coexpression and circadian-timed activation of kisspeptin and RFRP-3 neurons may contribute to the sexually dimorphic basis of the LH surge. *Endocrinology* **158** 3565–3578. (https://doi.org/10.1210/en.2017-00405)

Rebuli ME & Patisaul HB 2016 Assessment of sex specific endocrine disrupting effects in the prenatal and pre-pubertal rodent brain. *Journal of Steroid Biochemistry and Molecular Biology* **160** 148–159. (https://doi.org/10.1016/j.jsbmb.2015.08.021)

Schambra U 2008 *Prenatal Mouse Brain Atlas: Color Images and Annotated Diagrams of: Gestational Days 12, 14, 16 and 18 Sagittal, Coronal and Horizontal Section*. Berlin, Germany: Springer Sciences and Business Media.

Smith JT, Cunningham MJ, Rissman EF, Clifton DK & Steiner RA 2005*a* Regulation of Kiss1 gene expression in the brain of the female mouse. *Endocrinology* **146** 3686–3692. (https://doi.org/10.1210/en.2005-0488)

Smith JT, Dungan HM, Stoll EA, Gottsch ML, Braun RE, Eacker SM, Clifton DK & Steiner RA 2005*b* Differential regulation of KiSS-1 mRNA expression by sex steroids in the brain of the male mouse. *Endocrinology* **146** 2976–2984. (https://doi.org/10.1210/en.2005-0323)

Treen AK, Luo V, Chalmers JA, Dalvi PS, Tran D, Ye W, Kim GL, Friedman Z & Belsham DD 2016 Divergent regulation of ER and Kiss genes by 17β-estradiol in hypothalamic ARC versus AVPV models. *Molecular Endocrinology* **30** 217–233. (https://doi.org/10.1210/me.2015-1189)

Wolfe CA, Van Doren M, Walker HJ, Seney ML, McClellan KM & Tobet SA 2005 Sex differences in the location of immunochemically defined cell populations in the mouse preoptic area/anterior hypothalamus. *Brain Research: Developmental Brain Research* **157** 34–41. (https://doi.org/10.1016/j.devbrainres.2005.03.001)

Yip SH, Boehm U, Herbison AE & Campbell RE 2015 Conditional viral tract-tracing delineates the projections of the distinct kisspeptin neuron populations to gonadotropin-releasing hormone (GnRH) neurons in the mouse. *Endocrinology* **156** 2582–2594. (https://doi.org/10.1210/en.2015-1131)

Young WJ & Chang C 1998 Ontogeny and autoregulation of androgen receptor mRNA expression in the nervous system. *Endocrine* **9** 79–88. (https://doi.org/10.1385/ENDO:9:1:79)

Received in final form 25 October 2019
Accepted 31 October 2019
Accepted Manuscript published online 31 October 2019